Toxicology in Vitro 36 (2016) 216–223

Contents lists available at ScienceDirect

Toxicology in Vitro

journal homepage: www.elsevier.com/locate/toxinvit

Oxidative stress generation of silver nanoparticles in three bacterial genera and its relationship with the antimicrobial activity

M.A. Quinteros [a,b], V. Cano Aristizábal [b], P.R. Dalmasso [d], M.G. Paraje [a,e], P.L. Páez [b,c,*]

[a] Instituto Multidisciplinario de Biología Vegetal (IMBIV), Consejo Nacional de Investigaciones Científicas y Técnicas (CONICET), Argentina
[b] Dto. Farmacia, Facultad de Ciencias Químicas, Universidad Nacional de Córdoba, Argentina
[c] Unidad de Tecnología Farmacéutica (UNITEFA), Consejo Nacional de Investigaciones Científicas y Técnicas (CONICET), Argentina
[d] CITSE, INBIONATEC, CONICET, Universidad Nacional de Santiago del Estero, RN 9, Km 1125, 4206 Santiago del Estero, Argentina
[e] Cátedra de Microbiología, Facultad de Ciencias Exactas Físicas y Naturales, Universidad Nacional de Córdoba, Argentina

ARTICLE INFO

Article history:
Received 24 May 2016
Received in revised form 11 August 2016
Accepted 12 August 2016
Available online 13 August 2016

Keywords:
Oxidative stress
Bacteria
Silver nanoparticles
Biosynthesis
Antimicrobial activity

ABSTRACT

Oxidative stress is a condition caused by the high intracellular concentrations of reactive oxygen species (ROS) that includes superoxide anion radicals, hydroxyl radicals and hydrogen peroxide. Nanoparticles could cause rapid generation of free radicals by redox reactions. ROS can react directly with membrane lipids, proteins and DNA and are normally scavenged by antioxidants that are capable of neutralizing; however, elevated concentrations of ROS in bacterial cells can result in oxidative stress. The aim of this work was contribute to the knowledge of action mechanism of silver nanoparticles (Ag-NPs) and their relation to the generation of oxidative stress in bacteria. We demonstrated that Ag-NPs generated oxidative stress in *Staphylococcus aureus*, *Escherichia coli* and *Pseudomonas aeruginosa* mediated by the increment of ROS and this increase correlated with a better antimicrobial activity. On the other hand, we showed that the oxidative stress caused by the Ag-NPs biosynthesized was associated to a variation in the level of reactive nitrogen intermediates (RNI). Oxidative stress in bacteria can result from disruption of the electronic transport chain due to the high affinity of Ag-NPs for the cell membrane. This imbalance in the oxidative stress was evidentiated by a macromolecular oxidation at level of DNA, lipids and proteins in *E. coli* exposed to Ag-NPs. The formation of ROS and RNI by Ag-NPs may also be considered to explain the bacterial death.

1. Introduction

The antibiotic-resistant pathogens pose a threat to the treatment of a wide range of severe infections and have demonstrated great success in its ability to develop resistance mechanisms, often transferable against virtually all antibiotics in clinical use (Gopal Rao, 1998). The emergence of bacterial strains resistant to many antibiotics currently used emphasizes the need for new approaches to treating infections.

It is increasingly common to hear the terms nanotechnology, nanomaterials, nanoparticles, etc., the impact is undeniable that the study of nanoscience and nanotechnology developments have on social, cultural and economic spheres of our daily life (Sharma et al., 2009). Due to the countless individuals and physicochemical properties, the metal nanoparticles have received attention for their multiple applications in different economic sectors, including electronics, pharmacy, medicine, energy, agriculture, etc. In this sense, silver nanoparticles could be used to increase the contrast of objects of interest in living systems, furthermore could be improved the design of the silver contrast agent to promote its biocompatibility and excretion (Karunamuni et al., 2016). On the other hand, it has been found that gold-silver alloy nanoparticles have potential for both blood pool imaging and breast cancer screening (Naha et al., 2016).

Thus, a key breakthrough that has experienced nanoscience and nanotechnology in recent year's aspect is the development of experimental synthesis protocols for obtaining fast and reliable way to nanoparticles range of chemistries, sizes and high monodispersity (Komarneni et al., 2002).

Silver nanoparticles have proven effective against antibiotic resistant bacteria (Quinteros et al., 2016). The antimicrobial properties of silver are attributed to their high reactivity with proteins, structural changes in the cell wall and the membrane, resulting in inhibition and cell death. Additionally they attach them high reactivity with bacterial DNA replication by inhibiting (Durán et al., 2016; Gambino and Cappitelli, 2016).

Metal nanoparticles could cause rapid generation of free radicals by redox reactions in which reacts with oxygen or water and free Fe^{2+} which then generates reactive oxygen species (ROS) via the Fenton

* Corresponding author at: Dpto. Farmacia, Facultad de Ciencias Químicas, Universidad Nacional de Córdoba, Haya de la Torre y Medina Allende, Ciudad Universitaria, X5000HUA Córdoba, Argentina.
E-mail address: plpaez@fcq.unc.edu.ar (P.L. Páez).

http://dx.doi.org/10.1016/j.tiv.2016.08.007
0887-2333/

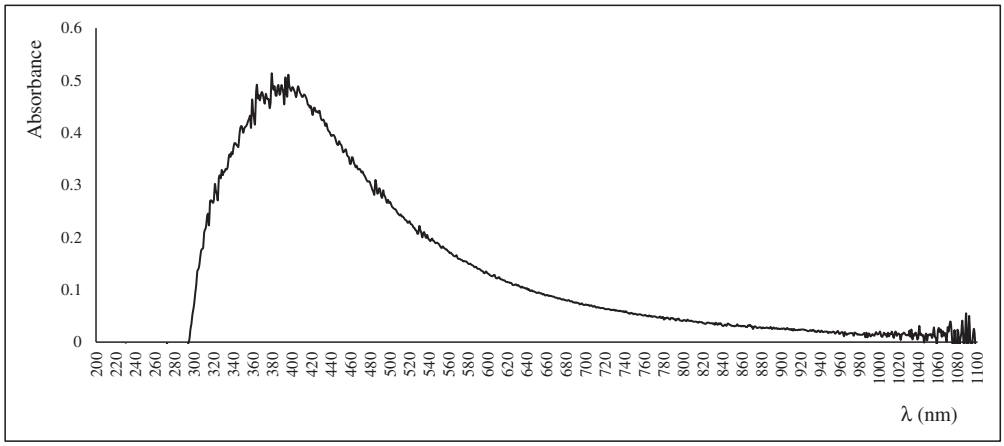

Fig. 1. UV–vis spectrum of Ag-NPs biosynthesized. The nanoparticles were obtained of *P. aeruginosa* ATCC 27853 supernatant.

reaction (Keenan and Sedlak, 2008). High concentrations of ROS in the cell can result in the generation of oxidative stress (Arce Miranda et al., 2011; Páez et al., 2011). Oxidative stress is a condition caused by the high intracellular concentrations of ROS that microbial cells are capable of neutralizing (Wang et al., 2004; Páez et al., 2009). ROS include superoxide radicals, hydroxyl radicals and hydrogen peroxide, among others. For example, ROS are normally produced during the metabolism of prokaryotic and eukaryotic mitochondria, chloroplasts, peroxisomes or in the cytosol, mainly as a byproduct of aerobic respiration (Arce Miranda et al., 2011; Asada, 2006). ROS production is initialized mainly extracellular sources such as ultraviolet light or transition metals, including iron (Villegas et al., 2013). It was found that when Fe_2O_3 nanoparticles to a cell culture were added ROS levels increased 50-fold (Limbach et al., 2007). Cells subjected to oxidative stress have various dysfunctions in the lipid membrane, protein and DNA which could result in death of the microorganisms (Davies, 2000). Hydroxyl radicals have the most deleterious impact on cell viability. To counteract oxidative stress, organisms have developed various protective mechanisms. The system response involves the production of repair enzymes and antioxidants (Thammavongs et al., 2008; Angel Villegas et al., 2015).

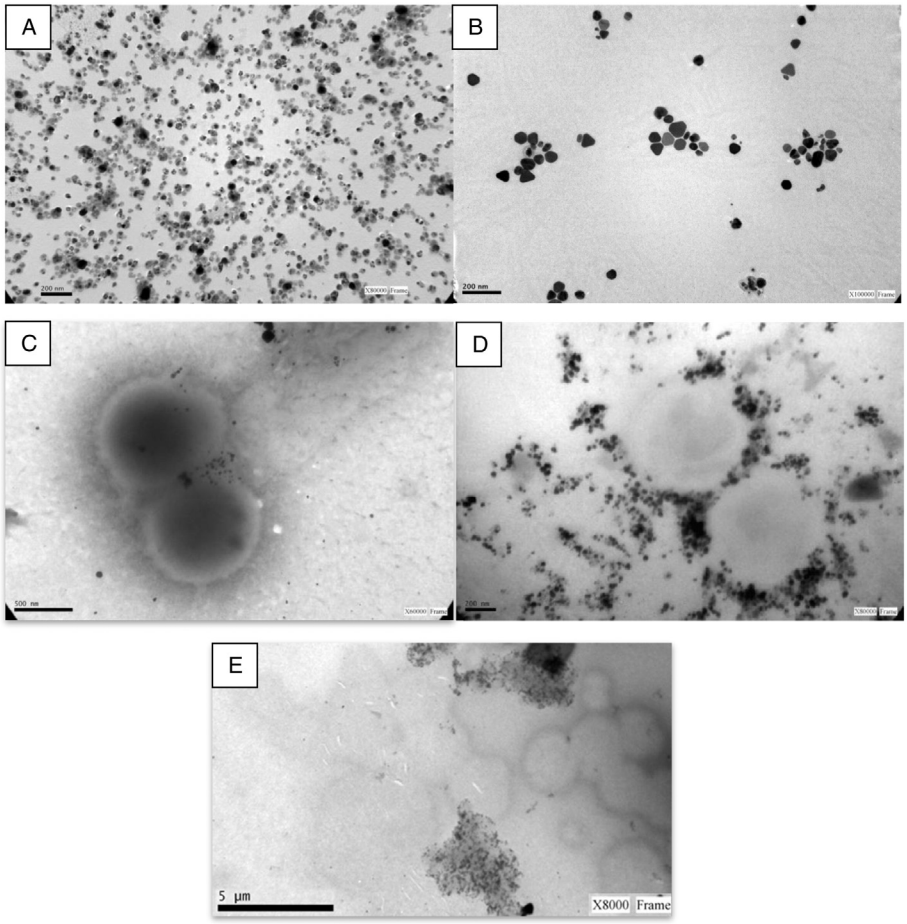

Fig. 2. Morphology characterization of Ag-NPs with TEM. (A and B) Silver nanoparticles biosynthesized. (C, D and E) *S. aureus* ATCC 29213 incubated with Ag-NPs for 0, 1 and 6 h, respectively.

Table 1
Antimicrobial activity shown by Ag-NPs, CIP and $AgNO_3$ against test bacteria.

Strains	Ag-NPs		CIP		$AgNO_3$	
	MIC (pM)	MBC (pM)	MIC (μM)	MBC (μM)	MIC (μM)	MBC (μM)
Staphylococcus aureus ATCC 29213	0.203	0.203	1.3	1.3	78	78
Escherichia coli ATCC 25922	0.101	0.101	0.3	0.3	78	78
Pseudomonas aeruginosa ATCC 27853	0.016	0.016	0.6	1.3	10	10

The aim of this work is i) to contribute to understanding of the mechanism of Ag-NPs action as generators of oxidative damage in different bacterial genera by assessing oxidative and nitrosative stress, and ii) to extend the existing scant information in the literature on Ag-NPs/bacteria interaction (Quinteros et al., 2016), as part of ongoing in our laboratory regarding the oxidative stress involved in the antibacterial action. We considered, based on the above background, the hypothesis that silver nanoparticles obtained by biosynthesis could interact with the bacterial membrane and altering the respiratory metabolism leading to cell to a condition of oxidative stress which lead to bacterial death of several species.

2. Materials and methods

2.1. Chemicals and reagents

H_2-DCFDA (6-carboxy-2′,7′-dichlorodihydrofluorescein diacetate diacetoximetil ester), and N-(1-naphthyl)ethylenediamine dihydrochloride were all obtained from Sigma-Aldrich (St. Louis, MO, USA). Other chemicals used were sulfanilamide (Merck, Darmstadt, Germany), Luria Bertani broth (MP Biomedicals, France), ciprofloxacin (CIP) (Prarfarm, Argentina), $AgNO_3$ (Ciccarelli, Argentina) and Mueller Hinton medium (Britania, Argentina).

2.2. Bacterial strains

Staphylococcus aureus ATCC 29213, *Escherichia coli* ATCC 25922, *Pseudomonas aeruginosa* ATCC 27853.

2.3. Biosynthesis of Ag-NPs

The Ag-NPs were prepared according to the described by Ahmad et al. (2003) with slight modifications. Luria Bertani broth was prepared, sterilized, and inoculated with a fresh growth of test strain. The cultured flasks were incubated at 37 °C for 24 h. After the incubation time, the culture was centrifuged at 10,000 rpm and the supernatant was used for the synthesis of Ag-NPs. *P. aeruginosa* culture supernatant was separately added to the reaction vessels containing silver nitrate at a concentration of 10 mM. The bioreduction of the Ag^+ ions in the solution was monitored by sampling the aqueous component (2 mL) and measuring the ultraviolet-visible (UV–vis) spectrum of the solution. UV–vis spectra of these samples were monitored on a Biotek Synergy 2 multimode microplate reader, operated at a resolution of 1 nm. Furthermore, the Ag-NPs were characterized by transmission electron microscopy (TEM) using a TEM Jeol, JEM1200 EXII, USA.

2.4. Susceptibility to Ag-NPs

Minimum inhibitory concentration (MIC) and bactericidal concentration (MBC) were determined by using the standard tube dilution method on Mueller Hinton (MH) broth in accordance with standards established by the Clinical and Laboratory Standards Institute (CLSI, 2011). An overnight culture of each microorganism was diluted to achieve a cell density in the range from 10^5 to 10^7 colonies forming units per milliliter (CFU/mL) and incubated for 10 min at 37 °C. The Ag-NPs, $AgNO_3$ or CIP were then added in serial dilutions. Bacterial growth was observed at 18 h of incubation. The cell suspension (0.5 mL) was inoculated into each tube to give a total volume of 1 mL.

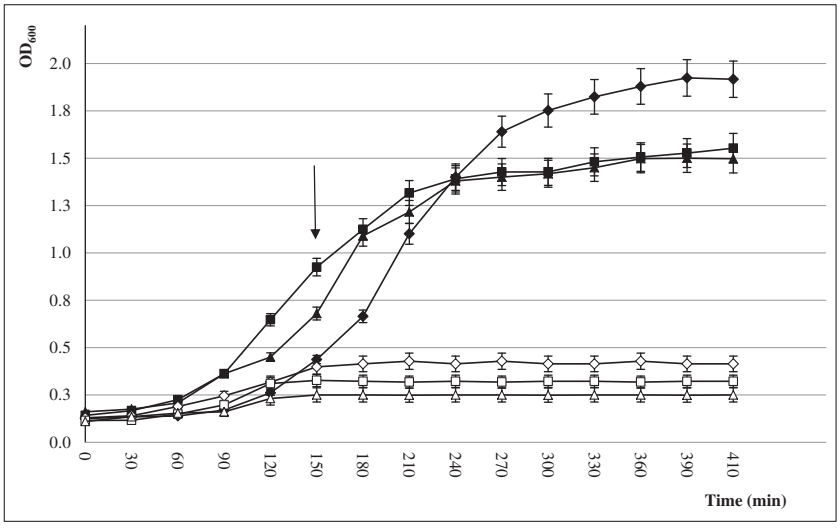

Fig. 3. Growth curves of *S. aureus*, *E. coli* and *P. aeruginosa*. The tree bacterial species assayed were inoculated to 150 min (arrow) with or without Ag-Nps 0.6 pM. *S. aureus* ATCC 29213 (♦), *E. coli* ATCC 25922 (■), *P. aeruginosa* ATCC 27853 (▲), *S. aureus* ATCC 29213 treated with Ag-NPs (◇), *E. coli* ATCC 25922 treated with Ag-NPs (□), *P. aeruginosa* treated with Ag-NPs (△).

The lowest concentration of the antimicrobial agent that prevented bacterial growth was considered to be the MIC. Viable bacterial counts were obtained for samples without visible bacterial growth by plating on MH agar plates, followed by aerobic incubation at 37 °C for 18 h. The antimicrobial agent concentration that produces the death of 99.9% of initial inoculum was considered the MBC. To quantify the effect of Ag-NPs on the bacterial growth, a time-response growth curve was obtained in the presence of nanoparticles. In brief, a single CFU of each reference strain was diluted in MH broth and grown for 18 h at 37 °C with constant agitation at 140 rpm. Then, each culture was adjusted to 0.5 index in McFarland scale and inoculated at a cell density of 10^6 CFU/mL in 2 mL of MH broth. For each strain culture was divided in two new cultures of 1 mL each. One culture received the antimicrobial compound and the control received phosphate buffer solution (PBS). The bacterial cultures were then incubated at 37 °C with constant agitation at 140 rpm. In different times, an aliquot of the broth was collected and the optical density at 600 nm (OD_{600}) was determined.

2.5. Determination of ROS by spectrofluorometry

Bacterial suspension (100 μL) were incubated with 100 μL of Ag-NPs (1.29 to 12.9 pM) at different times (1, 2, 3 and 4 h) at 37 °C. Then, 20 μL of H_2-DCFDA 20 μM aqueous solution were added. The fluorescence intensity was measured 30 min later with a spectrofluorometer Biotek Synergy HT with the excitation and emission wavelengths at 480 and 520 nm, respectively. Fluorescent microscopy was used as a monitor of intracellular ROS generation by using H_2-DCFDA using a NIKON TE-2000U microscope, (excitation, 490 nm; emission, 519 nm; mirror, 500 nm; emission, LP 515 nm) Japan (Peralta et al., 2015).

2.6. Quantification of reactive nitrogen intermediates (RNI) using the Griess's reaction

Nitric oxide (NO) is rapidly converted to nitrite in aqueous solutions and, therefore, the total nitrite can be used as an indicator of NO

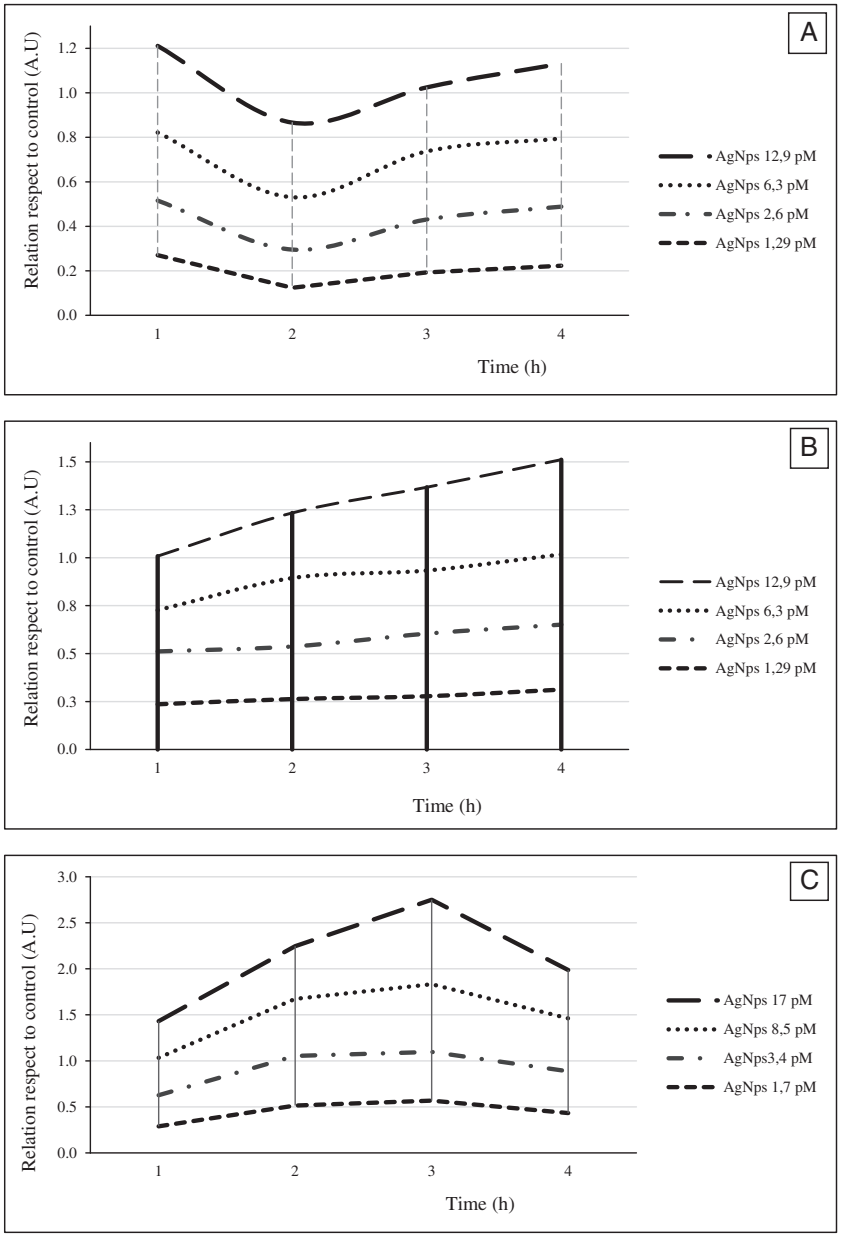

Fig. 4. Reactive oxygen species determined by spectrofluorometry with H_2-DCF in *S. aureus* (A), *E. coli* (B) and *P. aeruginosa* (C).

concentration. This was measured using a spectrophotometric analysis of the total nitrite performed by using Griess's reagent according to the methodology described by Kobayashi et al. (Galera et al., 2016; Baronetti et al., 2011). The bacterial suspension (100 μL) were incubated with 100 μL of Ag-NPs (2.1 to 21 pM) at different times (1, 2, 3 and 4 h) at 37 °C. Then, 50 μL of 2% sulfanilamide in 5% (v/v) HCl and 50 μL of 0.1% N-(1-naphthyl)ethylenediamine dihydrochloride aqueous solution were added. The formation of the azo dye was measured 15 min later by spectrophotometry at 540 nm. The OD was directly proportional to the nitrite content of the standard solution. Results were expressed respect to control without Ag-NPs.

2.7. DNA oxidation

The bacterial suspension ($OD_{600} = 1$) was incubated with 0.5 mL of Ag-NPs 15 pM by 4 h. Then, the DNA was purified according to the methodology described by Becerra et al. (2006) and oxidation of nucleoside dG was quantitated by HPLC. 1 mM of dG and 8-OHdG were applied as standards of non-oxidized and oxidized nucleoside, respectively. Results were expressed by the 8-OHdG/dG ratio.

2.8. Advanced oxidation protein products (AOPP)

0.5 mL of bacterial suspensions of *E. coli* ATCC 25922 cultured overnight in TSB at 35 °C were incubated with 0.5 mL of Ag-NPs 15 pM or phosphate saline buffer for 4 h. 0.1 mL of the samples was taken at 0 and 4 h of incubation. Then, 50 μL of IK (1.16 M) and 50 μL of acetic acid were added. The final product of the reaction was read at 340 nm, with chloramine-T (50 μM) being used as the standard. The concentrations of AOPP were expressed as chloramine-T equivalents per mg of proteins (Páez et al., 2011).

2.9. Lipid peroxidation

0.5 mL of bacterial suspension samples were incubated for 4 h with 0.5 mL of 15 pM Ag-NPs, or phosphate saline buffer (control). These incubations were stopped by employing 1 mL of trichloroacetic acid (TCA) 35% (p/v) in the absence of light. After, 1 mL of 0.5% thiobarbituric acid (TBA) was added and the samples were heated to 80 °C for 30 min. An ice bath was then used to cool the samples, after which, they were centrifuged and the absorbance of supernatant was determined at 535 nm. A calibration curve of MDA solutions was applied to estimate the lipid oxidation, with MDA levels expressed per mg of protein (nmol MDA/mgP) (Páez et al., 2011).

2.10. Statistical analysis

The assays were performed at least in triplicate in three independent assays. Data were expressed as means ± SD and analyzed by the Student's *t*-test. $P < 0.05$ was used as the level of statistical significance.

3. Results

3.1. Biosynthesis of Ag-NPs

Nanoparticles exhibited an absorption peak around 390 nm after 24 h of reaction (Fig. 1), which is a characteristic plasmon resonance surface of the band (SPR) of silver nanoparticles possibly due to excitation of longitudinal vibrations plasmon in nanoparticles silver in the solution. As visualized by TEM, Ag-NPs suspension appeared as a mixture of homogeneous particles by size and shape Fig. 2(A and B). Most particles were spherical, but the sporadic presence of regular polygonal particles was also observed. The Fig. 2(C, D and E) shows too the bactericidal activity of Ag-NPs in *S. aureus*. It can be seen how nanoparticles adhere to the wall of *S. aureus* after 1 h incubation while after 6 h incubation lysis of the bacteria was observed.

3.2. Susceptibility assays

MIC and MBC of Ag-NPs for the three bacterial species studied were ranged from 0.016 to 0.203 pM. The values of MIC and MBC for CIP were in order 0.3 to 1.3 μM while the values obtained for $AgNO_3$ were from 10 to 78 μM (Table 1).

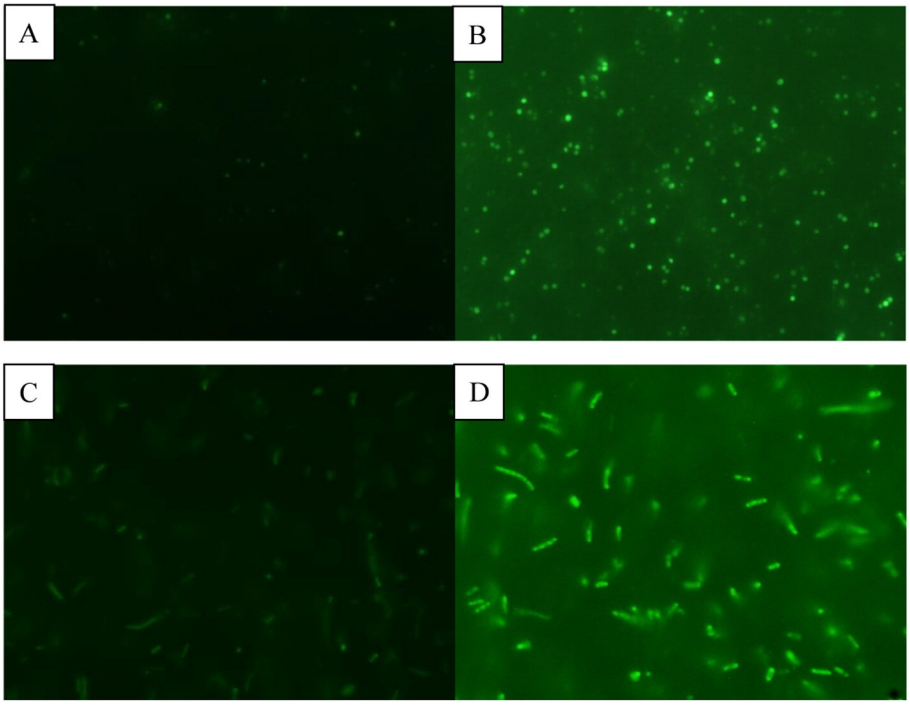

Fig. 5. Fluorescent microscopy obtained after incubation with Ag-NPs. (A) *S. aureus* control, (B) *S. aureus* after 1 h of incubation with Ag-NPs. (C) *E. coli* control, (D) *E. coli* after 4 h of incubation with Ag-NPs. Magnification 40× and scale bar is 10 μm.

Fig. 3 shows that the Ag-NPs reduced drastically the OD of the bacterial suspension over 5 h of incubation after adding Ag-NPs in the three bacterial genera studied respect to control. The OD_{600} with Ag-NPs treatment was about 4.5-fold lower than the control (without treatment) for *S. aureus* and *E. coli*, while 6-fold lower for *P. aeruginosa*.

3.3. Generation of oxidative stress by Ag-NPs

ROS generation induced by Ag-NPs was time and concentration dependent in the three bacterial species studied (Fig. 4). The increased ROS production in *S. aureus* was observed after 1 h incubation with Ag-NPs (1.29–12.9 pM) (Fig. 4-A) while at 2 h at the highest concentration of nanoparticles tested was reduced 20%. In *E. coli*, ROS generation was time-dependent with the maximum stimulation observed at 4 h of incubation with Ag-NPs (Fig. 4-B). Fig. 4-C shows the increase in ROS in *P. aeruginosa* until 3 h incubation with 17 pM of Ag-NPs, then a decline in ROS levels was observed at all concentrations of nanoparticles studied. These results were confirmed by fluorescence microscopy (Fig. 5).

3.4. Determination of RNI by Griess's reaction

Similarly to the determination of ROS production, the levels of RNI were time and dose-dependent when the bacterial strains tested were incubated with Ag-NPs (Fig. 6). In *S. aureus* (Fig. 6-A), the maximum stimulus was obtained after 2 h while the RNI generation in *E. coli* was lower at this time of incubation with the nanoparticles (Fig. 6-B). Fig. 5-C shows that in *P. aeruginosa*, the RNI values decreased with time a 20% until 2 h and then, remain constants.

3.5. Macromolecular oxidation generated by Ag-NPs

An important augment in the oxidation of ADN, lipids and protein was observed in *E. coli* incubated with Ag-NPs as a consequence of ROS increment. Table 2 shows an increment of 60% in the oxidation of the three macromolecules evaluated respect to control without nanoparticles.

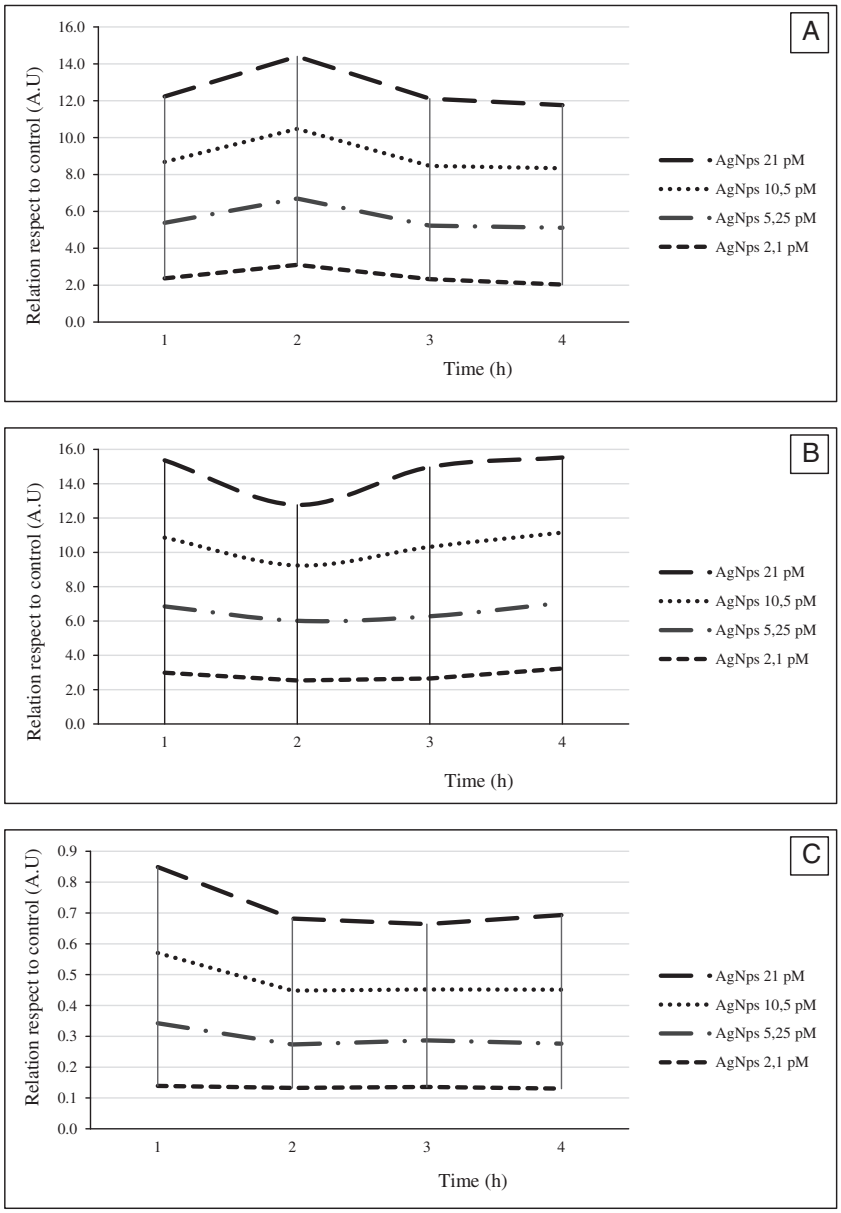

Fig. 6. Reactive nitrogen intermediates determined by Griess's reaction in *S. aureus* (A), *E. coli* (B) and *P. aeruginosa* (C).

Table 2
Macromolecular oxidation generated by Ag-NPs in *E. coli*.

	OH-dG/dG	nmol MDA/mgP	meq chloramine-T/mgP
Control	0.87	15.5	2.8
Ag-NPs	1.39*	24.8*	4.5*

* $P < 0.05$ respect to control without Ag-NPs.

4. Discussion

Continuous selections of bacteria that are resistant to a wide range of antibiotics have determined the necessity to discover new unconventional sources of antimicrobials (Cardozo et al., 2013). The generation of new compounds obtained by biosynthesis, ecofriendly, effective and inexpensive against these resistant bacteria may be a solution to this global problem. The results obtained in this work suggest that *P. aeruginosa*-produced Ag-NPs have bactericidal effects against *S. aureus*, *E. coli* and *P. aeruginosa* and may be an alternative treatment to the infections caused by these microorganisms. It has been found that many compounds of biological (Cardozo et al., 2013; Comini et al., 2011; Nhiem et al., 2010) and chemical (Páez et al., 2013) synthesis have antimicrobial activity against various microorganisms of clinical importance. In this sense, we have achieved a biosynthetic product with the advantages that this represents, which has a significant bactericidal activity against *S. aureus*, *E. coli* and *P. aeruginosa*. The antibacterial activity of Ag-NPs obtained by biosynthesis was in the order of pM and represents a concentration well below that those concentrations of antibiotics clinically used against these microorganisms.

Auffan et al. (Auffan et al., 2008) examined the effect of 1 h exposure to a type of mutants of *E. coli* for Fe_2O_3 nanoparticles. In that study, TEM showed morphological changes of bacterial cells and also changes the shape of the nanoparticle. The authors suggest that nanoparticles could cause oxidative stress through the generation of ROS and the Fenton reaction, as demonstrated using a mutant strain of *E. coli* without protection SOD. We show that Ag-NPs biosynthesized produced an increase of ROS in the three bacterial species assayed respect to control by spectrofluorometry and fluorescent microscopy.

In general, ROS and RNI can interact with numerous targets, including thiols, metal centers, tyrosine residues in proteins, nucleotide bases, and lipids. NO directly affects the activity of enzymes that inhibit bacterial respiration, growth arrest in *E. coli* and the suppression of DNA synthesis. Bacteria have specific and general defense strategies to counter environmental changes, including detoxification of stressors, as well as protection mechanisms and repair systems (Hochgräfe et al., 2008). The oxidative stress generated by Ag-NPs was associated to a reduction in the levels of RNI which is similar to the effect of different antibiotics in bacteria (Angel Villegas et al., 2015; Galera et al., 2016). Given that nanoparticles could exert their toxic effect on bacterial structures and various antibiotics act by oxidative mechanisms which lead to an oxidation of macromolecules like lipids, DNA and proteins and consequently, the bacterial death (Quinteros et al., 2016; Kohanski et al., 2007). Similar results were demonstrated by Naha et al. with polymeric nanoparticles which produce DNA damage dependent of intracellular ROS level (Naha and Byrne, 2013).

We were able to show that the Ag-NPs biosynthesized generated oxidative stress in *S. aureus*, *E. coli* and *P. aeruginosa* mediated by the increment of ROS and a reduction of RNI. The modification in the oxidative and nitrosative stress was too associated with a different antibacterial activity of the Ag-NPs against the three bacterial species tested.

Transparency document

The Transparency document associated with this article can be found, in the online version.

Acknowledgements

The authors thank to Consejo Nacional de Investigaciones Científicas y Técnicas de Argentina (CONICET) (PIP 11220130100702CO), Secretaría de Ciencia y Técnica de la Universidad Nacional de Córdoba (SECyT) (30820130100009CB) and Agencia Nacional de Promoción Científica y Tecnológica (ANPCyT) (PICT 2014 N° 1663) for financial support. We thank Silvana Ceballos for revision of this manuscript. Paulina L. Páez, María G. Paraje and Pablo R. Dalmasso are members of the Research Career of CONICET. Melisa Quinteros is PhD fellow of CONICET.

References

Ahmad, A., Mukherjee, P., Senapati, P., Mandal, D., Islam Khan, M., Kumar, R., Sastry, M., 2003. Extracellular biosynthesis of silver nanoparticles using the fungus *Fusarium oxysporum*. Colloids Surf. B 28, 313–318.
Angel Villegas, N., Baronetti, J., Albesa, I., Etcheverría, A., Becerra, M.C., Padola, N.L., Paraje, M.G., 2015. Effect of antibiotics on cellular stress generated in Shiga toxin-producing *Escherichia coli* O157:H7 and non-O157 biofilms. Toxicol. in Vitro 29, 1692–1700.
Arce Miranda, J.E., Sotomayor, C.E., Albesa, I., Paraje, M.G., 2011. Oxidative and nitrosative stress in *Staphylococcus aureus* biofilm. FEMS Microbiol. Lett. 315, 23–29.
Asada, K., 2006. Production and scavenging of reactive oxygen species in chloroplasts and their functions. Plant Physiol. 141, 391–396.
Auffan, M., Achouak, W., Rose, J., Roncato, M.A., Chaneiac, C., Waite, D.T., et al., 2008. Relation between the redox state of iron-based nanoparticles and their cytotoxicity toward *Escherichia coli*. Environ. Sci. Technol. 42, 6730–6735.
Baronetti, J.L., Angel Villegas, N., Paraje, M.G., Albesa, I., 2011. Nitric oxide-mediated apoptosis in rat macrophages subjected to Shiga toxin 2 from *Escherichia coli*. Microbiol. Immunol. 55, 231–238.
Becerra, M.C., Páez, P.L., Laróvere, L.E., Albesa, I., 2006. Lipids and DNA oxidation in *Staphylococcus aureus* as a consequence of oxidative stress generated by ciprofloxacin. Mol. Cell. Biochem. 285, 29–34.
Cardozo, V.F., Oliveira, A.G., Nishio, E.K., et al., 2013. Antibacterial activity of extracellular compounds produced by a *Pseudomonas* strain against methicillin-resistant *Staphylococcus aureus* (MRSA) strains. Ann. Clin. Microbiol. Antimicrob. 12, 12–19.
CLSI (Clinical and Laboratory Standards Institute), 2011. Methods for Dilution Antimicrobial Susceptibility Tests for Bacteria That Grow Aerobically. Approved Standard, M07-A8. 8. CLSI, Wayne, PA, USA.
Comini, L.R., Montoya, S.C., Páez, P.L., Argüello, G.A., Albesa, I., Cabrera, J.L., 2011. Antibacterial activity of anthraquinone derivatives from *Heterophyllaea pustulata* (Rubiaceae). J. Photochem. Photobiol. B 102, 108–114.
Davies, K.J., 2000. Oxidative stress, antioxidant defenses, and damage removal, repair, and replacement systems. IUBMB Life 50, 279–289.
Durán, N., Durán, M., Bispo de Jesus, M., Seabra, A.B., Fávaro, W.J., Nakazato, G., 2016. Silver nanoparticles: a new view on mechanistic aspects on antimicrobial activity. Nanomedicine 12, 789–799.
Galera, I.L.D., Paraje, M.G., Páez, P.L., 2016. Relationship between oxidative and nitrosative stress induced by gentamicin and ciprofloxacin in bacteria. J. Biol. Nat. 5, 122–130.
Gambino, M., Cappitelli, F., 2016. Mini-review: biofilm responses to oxidative stress. Biofouling 32, 167–178.
Gopal Rao, G., 1998. Risk factors for the spread of antibiotic-resistant bacteria. Drugs 55, 323–330.
Hochgräfe, F., Wolf, C., Fuchs, S., Liebeke, M., Lalk, M., Engelmann, S., Hecker, M., 2008. Nitric oxide stress induces different responses but mediates comparable protein thiol protection in *Bacillus subtilis* and *Staphylococcus aureus*. J. Bacteriol. 190, 4997–5008.
Karunamuni, R., Naha, P.C., Lau, K.C., Al-Zaki, A., Popov, A.V., Delikatny, E.J., Tsourkas, A., Cormode, D.P., Maidment, A.D.A., 2016. Development of silica-encapsulated silver nanoparticles as contrast agents intended for dual-energy mammography. Eur. Radiol. 26, 3301–3309.
Keenan, C.R., Sedlak, D.L., 2008. Factors affecting the yield of oxidants from the reaction of nanoparticulate zero-valent iron and oxygen. Environ. Sci. Technol. 42, 1262–1267.
Kohanski, M.A., Dwyer, D.J., Hayete, B., et al., 2007. A common mechanism of cellular death induced by bactericidal antibiotics. Cell 130, 797–810.
Komarneni, S., Li, D., Newalkar, B., Katsuki, H., Bhalla, A.S., 2002. Microwave–polyol process for Pt and Ag nanoparticles. Langmuir 18, 5959–5962.
Limbach, L.K., Wick, P., Manser, P., Grass, R.N., Bruinink, A., Stark, W.J., 2007. Exposure of engineered nanoparticles to human lung epithelial cells: influence of chemical composition and catalytic activity on oxidative stress. Environ. Sci. Technol. 41, 4158–4163.
Naha, P.C., Byrne, H.J., 2013. Generation of intracellular reactive oxygen species and genotoxicity effect to exposure of nanosized polyamidoamine (PAMAM) dendrimers in PLHC-1 cells in vitro. Aquat. Toxicol. 132–133, 61–72.
Naha, P.C., Lau, K.C., Hajfathalian, M., Mian, S., Chhour, P., Uppuluri, L., McDonald, E.S., Maidment, A.D., Cormode, D.P., 2016. Gold silver alloy nanoparticles (GSAN): an imaging probe for breast cancer screening with dual-energy mammography or computed tomography. Nanoscale 8 (28), 13740–13754.
Nhiem, T., Aparna, M., Dhriti, M., et al., 2010. Bactericidal effect of iron oxide nanoparticles on *Staphylococcus aureus*. Int. J. Nanomedicine 5, 277–283.
Páez, P.L., Becerra, M.C., Albesa, I., 2009. Antioxidative mechanisms protect resistant strains of *Staphylococcus aureus* against ciprofloxacin oxidative damage. Fundam. Clin. Pharmacol. 24, 771–776.

Páez, P.L., Becerra, M.C., Albesa, I., 2011. Comparison of macromolecular oxidation by reactive oxygen species in three bacterial genera exposed to different antibiotics. Cell Biochem. Biophys. 61, 467–472.

Páez, P.L., Bazán, C.M., Bongiovanni, M.E., Toneatto, J., et al., 2013. Oxidative stress and antimicrobial activity of chromium(III) and ruthenium(II) complexes on *Staphylococcus aureus* and *Escherichia coli*. Biomed Res. Int. 2013 (2013), 906912. http://dx.doi.org/10.1155/2013/906912.

Peralta, M.A., da Silva, M.A., Ortega, M.G., Cabrera, J.L., Paraje, M.G., 2015. Antifungal activity of a prenylated flavonoid from *Dalea elegans* against *Candida albicans* biofilms. Phytomedicine 22, 975–980.

Quinteros, M.A., Aiassa Martínez, I.M., Dalmasso, P.R., Páez, P.L., 2016. Silver nanoparticles: biosynthesis using an ATCC reference strain of *Pseudomonas aeruginosa* and activity as broad spectrum clinical antibacterial agents. Int. J. Biomater. 2016, 5971047. http://dx.doi.org/10.1155/2016/5971047.

Sharma, V.K., Yngard, R.A., Lin, Y., 2009. Silver nanoparticles: green synthesis and their antimicrobial activities. Adv. Colloid Interf. Sci. 145, 83–96.

Thammavongs, B., Denou, E., Missous, G., Gueguen, M., Panoff, J.M., 2008. Response to environmental stress as a global phenomenon in biology: the example of microorganisms. Microbes Environ. 23, 20–23.

Villegas, N.A., Baronetti, J., Albesa, I., Polifroni, R., Parma, A., Etcheverría, A., Becerra, M.C., Padola, N., Paraje, M.G., 2013. Relevance of biofilms in the pathogenesis of Shiga-toxin-producing *Escherichia coli* infection. Sci. World J. 2013, 607258. http://dx.doi.org/10.1155/2013/607258 (eCollection 2013).

Wang, Y., Leung, P.C., Qian, P., Gu, J.D., 2004. Effects of UV, H_2O_2 and Fe^{3+} on the growth of four environmental isolates of *Aeromonas* and *Vibrio* species from a mangrove environment. Microbes Environ. 19, 163–171.